Diblock Copolymer Templated Nanohybrid Thin Films of Highly Ordered TiO2 Nanoparticle Arrays in PMMA Matrix

ARTICLE *in* CHEMISTRY OF MATERIALS · NOVEMBER 2006

Impact Factor: 8.35 · DOI: 10.1021/cm061495f

6 AUTHORS, INCLUDING:

Akhmad Herman Yuwono
University of Indonesia
40 PUBLICATIONS **420** CITATIONS
SEE PROFILE

Yu Zhang
Autonomous University of Barcelona
45 PUBLICATIONS **550** CITATIONS
SEE PROFILE

John Wang
University of California, Irvine
235 PUBLICATIONS **3,773** CITATIONS
SEE PROFILE

Diblock Copolymer Templated Nanohybrid Thin Films of Highly Ordered TiO_2 Nanoparticle Arrays in PMMA Matrix

Akhmad Herman Yuwono,[†] Yu Zhang,[†] John Wang,*[,†] Xin Hai Zhang,[‡] Haiming Fan,[§] and Wei Ji[§]

Department of Materials Science and Engineering, Faculty of Engineering, National University of Singapore, Block EA #07-40, 9 Engineering Drive 1, Singapore 117576, Institute of Materials Research and Engineering, 3 Research Link, Singapore 117602, and Department of Physics, Faculty of Science, National University of Singapore, Block S12, 2 Science Drive 3, Singapore 117542

Received June 28, 2006. Revised Manuscript Received September 4, 2006

Solvent modification with a mixture of tetrahydrofuran and water in a proportional volume ratio of 50% has been employed to enable poly(methylmethacrylate)-*b*-polyethylene oxide diblock copolymer to be used as a template for preparing nanohybrid thin films containing highly ordered arrays of titanium dioxide (TiO_2) nanoparticles. With control of the processing parameters involved in the block copolymer templating, nanoarrays consisting of nanocrystalline TiO_2 particles were successfully assembled in the hexagonal-like or cubical-like hierarchical structures, as revealed by TEM studies. The phases and chemical nature of the titania nanoparticles have been confirmed by Raman and XPS spectroscopies. A significant enhancement in nanocrystallinity of the TiO_2 phase in the nanohybrid thin films was achieved by the application of an appropriate hydrothermal treatment in high-pressure water vapor at 150 °C. The nanocrystallinity strongly affects the UV absorbance and photoluminescence emission of the nanohybrid thin films.

Introduction

Highly ordered arrays of functional nanostructures derived from block copolymer templating are critically important for a number of technologically demanding applications, as almost all the optoelectronic, micromechanical, and biomedical devices are being miniaturized. Accordingly, several novel synthesis routes leading to the highly ordered arrays of TiO_2 nanoparticles by diblock copolymer templating have been reported, including polystyrene-*b*-poly(methylmethacrylate) (PS-*b*-PMMA),[1] polystyrene-*b*-polyethylene oxide (PS-*b*-PEO),[2−5] and more recently polystyrene-*b*-poly(2-vinylpyridine) (PS-*b*-P2VP).[6] When dissolved in a selected solvent at above their critical micelle concentrations, these diblock copolymers can easily form well-arranged inverse micelles, which function as nanoscopic reaction sites for formation of TiO_2 nanoparticles through hydrolysis/condensation, mineralization, or vapor deposition of the precursors.

However, the successful use of poly(methylmethacrylate)-*b*-polyethylene oxide (PMMA-*b*-PEO) block copolymer for templating the growth of titania nanoparticles has yet been reported. This is due to the difficulty of finding a selective solvent for this block copolymer that can favor the formation of micelle/inverse micelle. As reported by Edelmann et al.,[7] the solubility parameters of both PMMA and PEO are similar in most of the commercially available solvents, such as tetrahydrofuran (THF), acetone, and toluene, making the Flory−Huggins segmental interaction parameters (χ) for both polymer blocks nearly equal to each other and thus against micelle formation. This is a consequence of the strongly swollen PMMA chains of high mobility in those solvents.

Our previous study has shown that the nanohybrid thin films consisting of TiO_2 nanoparticles in PMMA derived from in situ sol−gel and polymerization routes are promising as a class of new nonlinear optical materials since they demonstrate a very fast recovery time of ∼1.5 ps and a large third-order nonlinear optical susceptibility, $\chi^{(3)}$ up to 1.93×10^{-9} esu.[8a,b] However, these existing synthesis routes often lead to a lack of uniformity in the inorganic−organic nanostructures, due to the condensation reaction involved in the hydrolyzed TiO_2 precursors, which takes place in random locations in the amorphous polymer matrix. Therefore, it will be of considerable interest to synthesize a nanohybrid where the formation sites for TiO_2 nanoparticles in the PMMA matrix can be controlled, for example, by block copolymer templating. In this paper, we report a

* To whom correspondence should be addressed. Phone: (65) 65161268. Fax: (65) 67763604. E-mail: msewangj@nus.edu.sg.

[†] Department of Materials Science and Engineering, Faculty of Engineering, National University of Singapore.

[‡] Institute of Materials Research and Engineering.

[§] Department of Physics, Faculty of Science, National University of Singapore.

(1) Weng, C. C.; Wei, K. H. *Chem. Mater.* **2003**, *15*, 2936.
(2) Spatz, J.; Mössmer, S.; Möller, M.; Kocher, M.; Neher, D.; Wegner, G. *Adv. Mater.* **1998**, *10*, 473.
(3) Sun, Z.; Gutmann, J. S. *Physica A* **2004**, *339*, 80.
(4) Kim, D. H.; Kim, S. H.; Lavery, K.; Russel, T. P. *Nano Lett.* **2004**, *4* (10), 1841.
(5) Kim, D. H.; Sun, Z.; Russel, T. P.; Knoll, W.; Gutmann, J. S. *Adv. Funct. Mater.* **2005**, *15*, 1160.
(6) Li, X.; Lau, K. H. A.; Kim, D. H.; Knoll, W. *Langmuir* **2005**, *21*, 5212.
(7) Edelmann, K.; Janich, M.; Hoinkis, E.; Pyckhout-Hintzen, W.; Höring, S. *Macromol. Chem. Phys.* **2001**, *202*, 1638.
(8) (a) Yuwono, A. H.; Xue, J. M.; Wang, J.; Elim, H. I.; Ji, W.; Li, Y.; White, T. J. *J. Mater. Chem.* **2003**, *13*, 1475. (b) Elim, H. I.; Ji, W.; Yuwono, A. H.; Xue, J. M.; Wang, J. *Appl. Phys. Lett.* **2003**, *82* (16), 2691.

10.1021/cm061495f CCC: $33.50
Published on Web 11/17/2006

templating route by making use of PMMA−PEO diblock copolymer for preparing nanohybrid thin films with well-organized patterns of TiO_2 nanoparticles. The synthesis process involves the dissolution of PMMA−PEO copolymer in a mixture solvent of THF and water, followed by incorporation of titanium alkoxide as the inorganic precursor into the hydrophilic sites. Although a similar process of incorporating titanium oxide by sol−gel chemistry coupled with PS-*b*-PMMA or PS-*b*-PEO diblock copolymer templating has been attempted by several researchers,[1−3,5] the present work is emphasized more specifically on an investigation into compromising the two contradicting aspects encountered in the templating with PMMA-*b*-PEO diblock copolymer, i.e., a huge amount of water in the solvent mixture, which is essential for micellization of PMMA−PEO blocks, and the highly water-sensitive nature of titanium alkoxides. In particular, we have found that both an appropriate water content and a low pH value of the mixture solvent are required to enable a nanohybrid thin film containing highly ordered arrays of TiO_2 nanoparticles in PMMA matrix. In addition, the effects of several other synthesis parameters, including the annealing rate, temperature, and holding time, on the resulting TiO_2−PMMA nanohybrid structures are investigated. We further demonstrate that a post-hydrothermal treatment with high-pressure water vapor is effective in enhancing the nanocrystallinity of TiO_2 nanoparticles. The nanostructures, phases, chemical bonding, and optical properties for both the conventionally annealed and post-hydrothermally treated nanohybrid thin films were studied and compared by using transmission electron microscopy (TEM), X-ray photoelectron spectroscopy (XPS), Fourier transform infrared (FTIR), UV−vis, and photoluminescence (PL) spectroscopies.

Experimental Section

Preparation of Nanohybrid Thin Films. PMMA-*b*-PEO diblock copolymer (12.5 mg) (Polymer Sources Inc; M_n PMMA:PEO = 1700:3500 g/mol and polydispersity of 1.1) was first dissolved in 2.5 mL of THF (99%, Acros) and stirred for 1 h. The solution appeared turbid, indicating that only the hydrophobic PMMA blocks had already been dissolved, while the hydrophilic PEO blocks still remained as a solid phase. Following Edelmann's work,[7] we modified the solvent by adding varying amounts of deionized water from 10 to 60 vol % into the solution. Upon the addition of deionized water, the solution turned clear, which was further stirred overnight. To compensate for the presence of high water content, the solution was purposely adjusted to be very acidic, i.e., pH 1.20, by adding several drops of hydrochloric acid (HCl, 37%, Aldrich). After the solution was stirred for 24 h, 25 mg of titanium tetraisopropoxide (TTIP, 98%, Acros) was added to the solution. Vigorous stirring for another 24 h led to complete dissolution of the precursor, resulting in a yellowish transparent solution. Two types of samples were prepared for study by using transmission electron microscopy (TEM): (i) by dropping a small amount of the solution onto a carbon-coated copper grid placed on tissue paper, leaving behind a thin film on the copper grid which was then annealed at the desired temperature, heating rate, and holding time; (ii) by scratching off the nanohybrid thin film spin-coated on the glass/quartz substrate by using a razor blade and then dispersing the debris into ethanol to make a suspension. A small amount of the suspension was then dropped carefully onto a carbon-coated copper grid, followed by drying.

Characterizations. TEM studies were conducted with a JEOL 3010 electron microscope operated at 300 keV and with a resolution of 0.14 nm. The thickness of the thin film spin-coated on the glass or quartz substrates was determined by using a surface profiler (Alpha-Step 500, Tencor). X-ray photoelectron spectroscopy (XPS) was acquired by using a VG Scientific ESCALAB MKII with a concentric hemisphere analyzer operated in the constant energy mode. A pass energy of 50 eV was employed for the wide scan survey spectrum while 20 eV was used for high-resolution core level scans. The exciting source was a Mg Kα operated at 150 W (10 mA; 15 kV) and the spectra were recorded using a 75° takeoff angle relative to the surface normal. All XPS core level spectra were fitted with XPSPEAK 4.1 program. The fitted XPS spectra were corrected for sample charging by applying a binding energy shift such that the hydrocarbon component of each C 1s region was centered at 285 eV. Raman spectroscopic study in this work was carried out in backscattering configuration by using a micro-Raman system (Renishaw 2000) with CCD detector. A diode pumped solid-state laser (DPSL) of 532 nm was employed as the excitation source, which was operated at a power rate of 10 mW. The laser beam was kept considerably low to avoid the undesired heating effects on the nanohybrid sample, where the spot size was controlled at approximately 1 μm. The spectral resolution of the apparatus is estimated to be approximately ~1 cm^{-1}. Infrared spectra of the nanohybrid thin films were recorded at room temperature in the range of 4000−400 cm^{-1}, by using a Varian 3100 FTIR Excalibur Series spectrometer, which has a resolution of ±4 cm^{-1}. Their absorption spectra were obtained by using a UV−vis spectrophotometer (UV-1601, Shimadzu) at the wavelength range of 800−200 nm with a resolution of ±0.3 nm. Photoluminescence (PL) measurement was performed with a micro-PL setup using a He−Cd laser operated at 325 nm as the excitation source. The laser beam was focused onto the sample surface by using an objective lens and the PL was collected through the same objective lens. The PL was dispersed in a monochromator and recorded using a CCD detector.

Results and Discussion

Water Content in the Solution. One of the primary concerns in the early stage of this investigation was the optimum water content that could enable PMMA−PEO diblock copolymer to be used as a template for the formation of highly ordered arrays of TiO_2 nanoparticles. As mentioned above, the desirable water content should be sufficiently large for the micellization of PMMA−PEO blocks, but on the other hand it should not exceed the limit beyond which the titanium alkoxide precursor would undergo a premature macro-precipitation. To prevent the latter, the solution was controlled at a considerably low pH level, i.e., pH ~ 1.20. Prior to investigation by using TEM, the film samples were annealed in air at 150 °C for 48 h at a heating rate of 1 °C/min. Figures 1a−1f show TEM images for the nanohybrid thin films derived from dissolution of PMMA−PEO diblock copolymer with different water contents. It is seen that a water content of 10 vol % resulted in a thin film containing nanoparticles distributed rather randomly, without any regular pattern formed (Figure 1a). Increasing the water content to 30 vol % leads to the formation of a slightly organized structure in the thin film, although some areas are still patternless (Figure 1b). In contrast, when the water content was further increased to 50 vol %, the resulting thin film

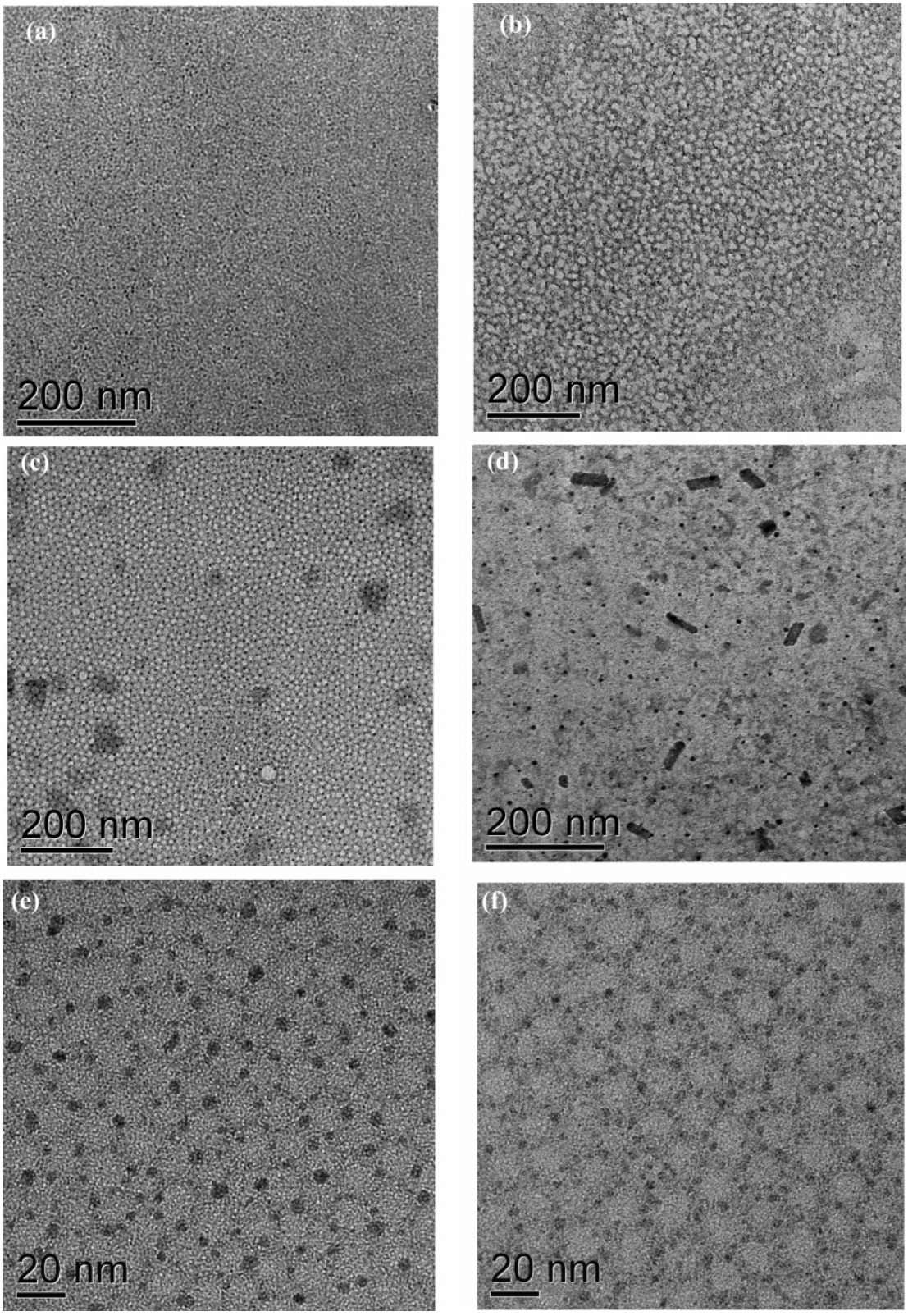

Figure 1. TEM micrographs of the thin films containing titania nanoparticles derived from dissolution of PMMA−PEO diblock copolymer in THF with water content of (a) 10, (b) 30, (c) 50, and (d) 60 vol %, respectively. High-magnification image of (c) is given in (e); (f) the nanohybrid thin film derived from the same conditions as (c) but spin-coated on the glass substrate.

demonstrates a much more regular array structure (Figure 1c), where clusters of fine titania particles were observed to form outside the spherical polymer (PMMA) domains of about 20 nm in diameter. Such an ordered structure shows that micelles consisting of hydrophilic PEO corona and hydrophobic PMMA core can be formed by controlling the processing parameters involved, where the synergistic micellization among PMMA−PEO chains is due to the reduced swelling and thus reduced mobility of PMMA, together with an increase in PEO mobility. [7] In addition to the clusters of fine TiO_2 particles, there also occur some relatively darker areas in Figure 1c, which indicate an inhomogeneity in the

distribution of TiO_2 precursor. Further increase in water content to 60 vol %, however, caused a premature precipitation of inorganic precursor, leading to the formation and severe aggregation of large titania crystallites, as shown in Figure 1d. As mentioned earlier, two types of TEM samples were prepared, namely, by dropping a small amount of the precursor solution onto a carbon-coated copper grid and by scratching off the nanohybrid thin film spin-coated on the glass/quartz substrate, respectively. To confirm the consistency in nanostructure between the two types of TEM samples prepared under the same annealing conditions, Figure 1f is a TEM micrograph for the thin film spin-coated on the glass substrate (3000 rpm for 20 s), which compares well with Figure 1e, which was for the sample directly deposited on carbon-coated copper grid.

When the hydrolyzing agents, i.e., water and hydrochloric acid, are attracted by the hydrophilic PEO domains, hydrolysis of titanium alkoxides in these hydrophilic sites resulted in the formation of fine TiO_2 particles, as shown by the TEM micrographs in Figures 1c, 1e, and 1f. However, X-ray diffraction for phase identification performed on the thin films coated on glass substrates did not show any noticeable peaks for titania in the 2θ range of 20−70°. The phenomenon could be accounted for by two considerations. First, there existed only a small amount of the nanoparticles in the very thin film sample. It was noted that the average thickness of the films spin-coated on the glass/quartz substrates, as determined by surface profiler, was <50 nm. Second, at the low annealing temperature of 150 °C, the hydrolyzed TiO_2 precursor was largely attached to PEO since a temperature of >250 °C is required to completely remove the organic template from the nanohybrid. As a consequence, the conversion from precursor to stoichiometric TiO_2 phase was hardly achieved at the low annealing temperature, and therefore these fine nanoparticles are largely amorphous. Given the fact that the nanocrystallinity of these fine TiO_2 crystallites in the nanohybrids is of short-range order, Raman spectroscopy, which works on the principle of inelastic scattering of photons, was employed to verify the nature of the inorganic phase. However, upon initial investigation with the thin film sample, the detected signal was very weak and meaningless. It was then realized that the nanohybrid thin film sample in this work was "too" transparent such that the laser light could largely pass through it; hence, no significant Raman scattering was generated. To overcome this limitation, nanohybrid films were scratched off from the substrates by using a razor blade. Accumulation of enough sample enabled us to obtain a meaningful Raman spectrum, which is given in Figure 2, where a considerably intense peak at 152 cm^{-1} is shown for the nanohybrid thin film, followed by four weak peaks at 203, 396, 508, and 628 cm^{-1}, respectively. The first two and the fifth peaks are in agreement with the E_g, Raman active mode of anatase phase (144, 197, and 639 cm^{-1}), while the third and fourth peaks can be assigned to the B_{1g} and A_{1g} or B_{1g} modes (399 and 513 or 519 cm^{-1}), respectively.[9] On the one hand, the well-resolved peak of the E_g mode at 152 cm^{-1} arises from the external vibration of anatase

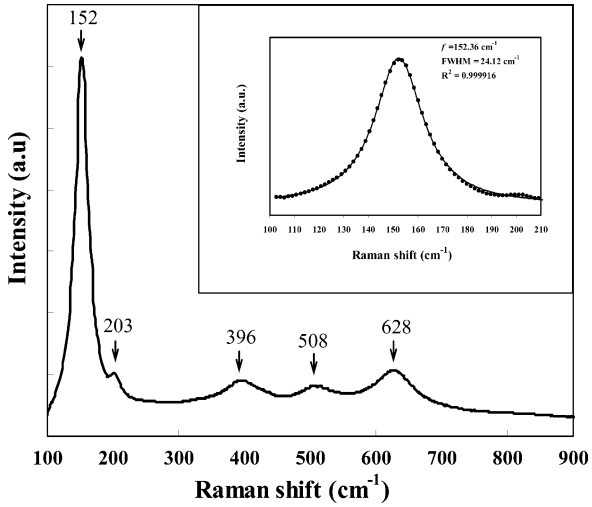

Figure 2. Raman spectroscopic spectrum of the nanohybrid thin film containing titania nanoparticle arrays in PMMA matrix, derived from the solution with water content of 50 vol % and pH 1.20.

structure,[10] confirming that fine anatase crystallites have indeed been formed in the nanohybrid structure. On the other hand, the intrinsically weak peak at 203 cm^{-1} and the broad bands at 396, 508, and 628 cm^{-1} agree with what has been shown by the XRD phase analysis; i.e., the crystallinity of the fine anatase particles is of short range. There is also a shift in wavenumber of the E_g mode to 152 cm^{-1}, with a broadened full-width at half-maximum (fwhm) of 24 cm^{-1} (inset of Figure 2), in comparison to 144 and 7 cm^{-1} in line width for single-crystal anatase.[10,11] A similar experimental result has been reported by Xu et al.[12] for the anatase titania nanoparticles coated with dodecylbenzenesulfonic acid (DBS/TiO_2) and stearic acid (St/TiO_2). The Raman shift is attributed to two likely phenomena in association with the nanoparticles: phonon confinement effect due to the decrease in particle dimension down to the nanometer scale and the strain applied by the surface coating. First, when phonons are effectively confined in space, their plane wave characters are lost and all the phonons over the Brillouin zone will contribute to the first-order Raman spectra. The weight of the off-center phonons increases as the crystallite size decreases, and the phonon dispersion results in an asymmetrical broadening and a shift of Raman peaks.[10] Second, a coating agent can provoke a compressive stress on the first several atom layers of TiO_2 nanoparticles and make the surface atoms pack closely, which in turn result in an increase in vibrational wavenumber.[12] In addition to these two considerations, a large contribution to the vibration spectra could also be due to the nonstoichiometry nature of the inorganic oxide nanoparticles, which is often the case for sol−gel-derived nanocrystalline systems. Parker and Siegel[13] have reported the role of O vacancies in generating a significant broadening and high-frequency shift in the main anatase band. By taking into account the fact that the titania nanoparticle arrays formed in the polymer matrix in this work are very small in size (<10 nm) and largely amorphous in

(9) Choi, H. C.; Jung, Y. M.; Kim, S. B. *Vib. Spectrosc.* **2005**, *37*, 33.
(10) Zhang, W. F.; He, Y. L.; Zhang, M. S.; Yin, Z.; Chen, Q. *J. Phys. D. Appl. Phys.* **2000**, *33*, 912.
(11) Bersani, D.; Lottici, P. P.; Ding, X. Z. *Appl. Phys. Lett.* **1998**, *72*, 73.
(12) Xu, C. Y.; Zhang, P. X.; Yan, L. *J. Raman Spectrosc.* **2001**, *32*, 862.
(13) Parker, J. C.; Siegel, R. W. *J. Mater. Res.* **1990**, *5*, 1246.

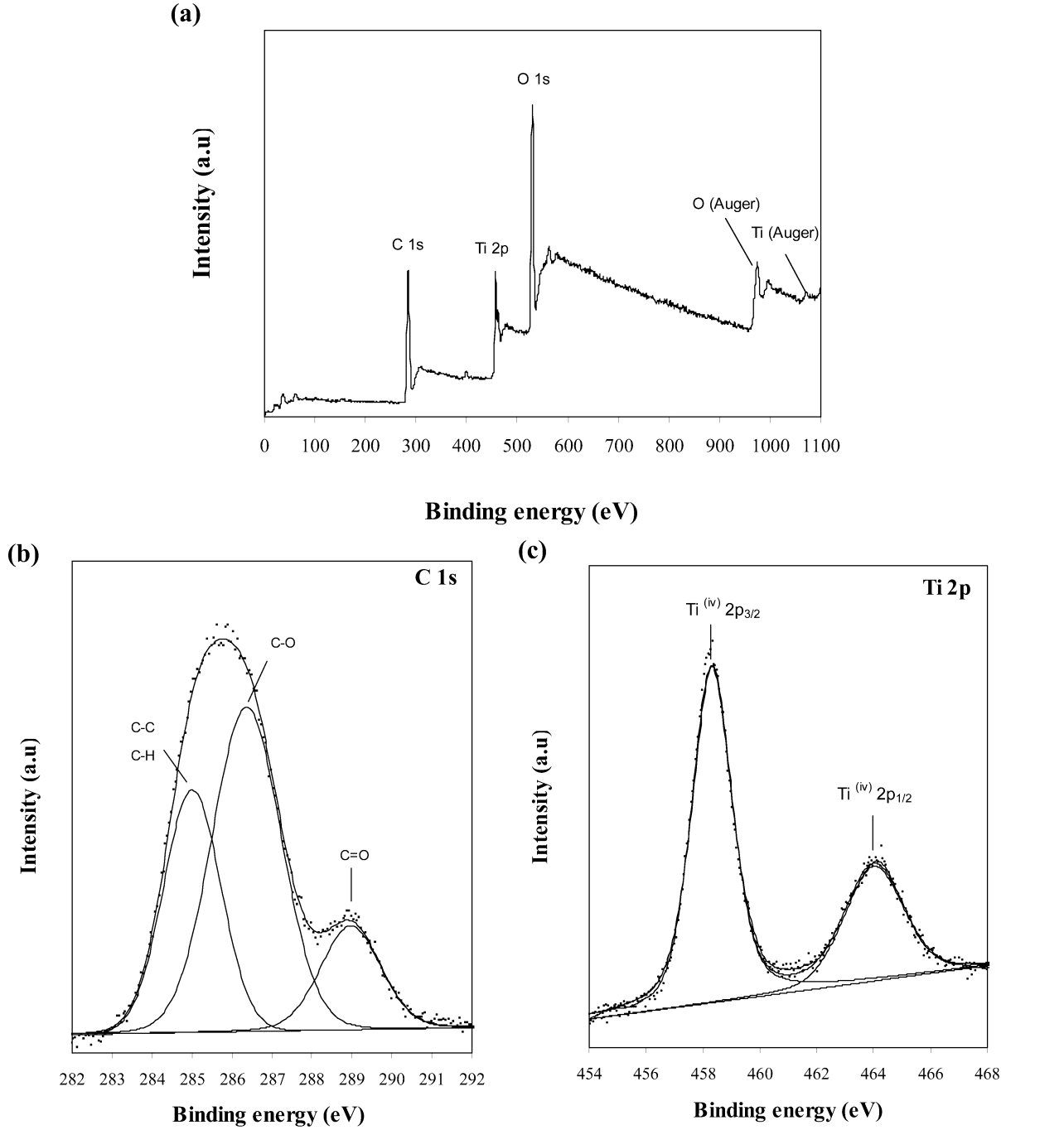

Figure 3. (a) Survey scan results of the XPS spectroscopy for the nanohybrid TiO_2−PMMA thin film, derived from the solution with water content of 50 vol % and pH 1.20; (b) high-resolution C 1s spectrum; and (c) high-resolution Ti 2p spectrum.

nature, which are also surrounded by abundant PMMA matrix, the observed Raman shift and peak broadening are thus expected. In the high spectral region (not shown here), the Raman spectrum shows peaks at ∼1459 and ∼2951 cm^{-1}, which can be assigned to CH_3 antisymmetric stretching, CH stretching, or CH_2 antisymmetric stretching from PMMA matrix.[14]

The chemical nature of the nanohybrid thin films was furthermore confirmed by X-ray photoelectron spectroscopy (XPS). Survey scan (Figure 3a) clearly shows the presence of C, Ti, and O on the film surface. O and Ti (Auger) also appear at higher binding energy levels in the spectrum, but they will not be taken into account in the following discussion. Figure 3b is the high-resolution C_{1s} spectrum, which apparently shows that it spans over a broad energy range from 293 to 281 eV, showing overlapping peaks due to the complex mixture of organic and inorganic carbon compounds involved. Curve fitting was therefore performed to deconvolute this spectrum and three individual peaks were obtained. The first peak at ∼284.80 eV is assigned to the adventitious carbon contamination which is unavoidably adsorbed from the atmosphere.[15] It is related to the fact that

(14) Park, B. J.; Sung, J. H.; Kim, K. S.; Chin, I.; Choi, H. J. *J. Macromol. Sci. Phys.* **2006**, *45*, 53.

(15) Yu, J. G.; Yu, J. C.; Zhao, X. J. *J. Sol−Gel. Sci. Technol.* **2002**, *24*, 95.

the samples were exposed to air before XPS experiments. Besides, the occurrence of elemental carbon can also be contributed to the existence of C−C and C−H bonds originating from the polymer matrix. Both of them are located at a very close binding energy of ∼285 eV.[16−19] Therefore, the overall peak does not appear as a sharp one; instead, it is rather broadened. Furthermore, the second and third peaks at 286.36 and 288.96 eV can be assigned to C−O and C═O bonds of the polymer matrix, respectively.[16,18] In addition, the C−O bonds in the nanohybrid thin films can also be contributed to the organic residues, such as alcohol and unhydrolyzed alkoxide groups of the inorganic precursor.[15]

Figure 3c reveals the characteristic doublet Ti $2p_{3/2}$ and Ti $2p_{1/2}$ at ∼458.29 and 464.01 eV, respectively. The area ratio of the two peaks, A(Ti $2p_{1/2}$)/A(Ti $2p_{3/2}$), is equal to 0.46 and the binding energy (BE) difference, $\Delta E_b = E_b$(Ti $2p_{1/2}$) − E_b(Ti $2p_{3/2}$), is 5.72 eV. All of these values are in a good agreement with the requirement for the valence state of Ti^{4+} in TiO_2 as reported in the literature.[20,21] It should be noted, however, there was a possibility that a certain amount of Ti_2O_3 species may be formed on the titania nanoparticle surfaces. This is so, by considering the fact that titania nanoparticles in the nanohybrids thin film are surrounded by the organic polymer matrix containing a huge number of residual elemental carbon and carbon bonds. The organic species during heat treatment took up oxygen, which could in turn enable the reduction of Ti^{4+} to Ti^{3+}.[22,23] Accordingly, a further fitting was performed by including two additional Ti 2p peaks for Ti_2O_3 species. However, the fitting result could not fulfill the difference in binding energy for Ti $2p_{3/2}$ and Ti $2p_{1/2}$ components of 5.70 eV as well as the ratio of 0.5 intensity ratio for the integrated area under both peaks. Garett and co-worker[24] compared the Ti 2p spectrum of a TiO_2 (110) single crystal with that of TiO_2 nanoparticle arrays synthesized via a nanosphere lithographic route. The evidence for Ti_2O_3 species in their case could be revealed only by a very slightly lower binding energy shoulder on the Ti $2p_{3/2}$ emission peak. They also found that quantization of the concentration of Ti^{3+} on the nanoparticles surface was intricate, due to the close proximity of the TiO_2 and Ti_2O_3 binding energies. It is well-known that the Ti^{3+} species are associated with corner, edge, or terrace defects on the surface sites. To be able to probe these surface Ti^{3+}defects, XPS spectra should be collected with photoelectrons of surface-sensitive takeoff angles. In this connection, Wang et al.[25] performed an XPS study on a TiO_2 (110) single crystal at takeoff angles of 15, 45, and 75° normal to the crystal surfaces. According to a previous work by Wandelt,[26] the XPS probing depths at 13 and 43° electron emission angles are ∼4 and ∼13 Å, respectively. Therefore, the spectrum collected at 15° can provide information on the uppermost layer of the single-crystal surface while that obtained at 75° represents the electronic bonding in the interior. Although significant differences could be observed among the O 1s spectra at the three takeoff angles, the Ti 2p spectra hardly change with the variation in emission angle. Shulz et al.[27] and Wang et al.[28] have reported the lack of change in the Ti 2p band as a result of the healing effect of the light-induced surface Ti^{3+} defects by adsorption species, such as oxygen and water. As a consequence, XPS is unable to distinguish among a defect-free surface, an oxygen-healed defective surface, and hydroxyl-healed defective surface in the Ti 2p region. With regard to these previous results, the XPS spectra in the present work were obtained at the 75° takeoff angle, where a substantial fraction of Ti_2O_3 species on the nanoparticle surfaces cannot be probed. Therefore, the Ti 2p spectra thus obtained only represented the valence state of Ti^{4+} in the TiO_2 lattice.

pH Value of Solution. The TEM results shown in Figures 1c, 1e, and 1f and the discussion above demonstrate that, in the solvent mixture each of 50 vol % water and THF, TiO_2 precursor species were taken up into the hydrophilic PEO sites, when the pH level of the precursor solution was adjusted to 1.20. This led to the formation of nanosized titania particle arrays without undergoing macroscale precipitation. However, as mentioned earlier, there also existed a number of locations where the titania nanoparticles were distributed rather unevenly. The average size of these nanoparticles was estimated to be 9 ± 1.5 nm. This suggests that, at the high water content of 50 vol %, which is in fact essential for micellization, the concentration of HCl in the solution was insufficient for a complete protonation of titanium alkoxide, resulting in so-called microaggregates to occur. The uneven aggregation was likely to occur when HCl was evaporated unavoidably and unevenly during the thermal annealing. This caused the PEO blocks to lose their ionic characters to some extent, increasing the compatibility of the constituent blocks, which in turn reduced the thermodynamic stability of the micelles.[2] To prevent such structural transformation, therefore, it is necessary to maintain a substantial amount of ions in the hydrophilic sites. To realize this, the solution was made more acidic by adjusting the pH value to as low as 0.33, while the other synthesis parameters were kept unchanged. As shown in Figure 4a, the resulting nanostructure shows no particle aggregation. A more interesting observation is that the film provides a highly dense and almost regular pattern resembling a "polycrystalline" morphology consisting of grains with different crystal orientations. Further TEM studies at higher magnification (Figure 4b) reveal that each small area consists of hexagonal-like arrays of PMMA cores

(16) Beamson, G.; Clark, D. T.; Law, D. S-L. *Surf. Interface Anal.* **1999**, *27*, 76.
(17) Zhu, Y. J.; Olson, N.; Beebe, T. P., Jr. *Environ. Sci. Technol.* **2001**, *35*, 3113.
(18) Que, W.; Zhou, Y.; Lam, Y. L.; Chan, Y. C.; Kam, C. H. *Appl. Phys. A* **2001**, *73*, 171.
(19) Gu, G. T.; Zhang, Z. J.; Dang, H. X. *Appl. Surf. Sci.* **2004**, *221*, 129.
(20) Pouilleau, J.; Devilliers, D.; Groult, H.; Marcus, P. *J. Mater. Sci.* **1997**, *32*, 5645.
(21) Kumar, P. M.; Badrinarayanan, S.; Sastry, M. *Thin Solid Films* **2000**, *358*, 122.
(22) Yu, J. G.; Zhao, X. J.; Zhao, Q. N. *Mater. Chem. Phys.* **2001**, *69*, 25.
(23) Yu, J. C.; Yu, J. G.; Tang, H. Y.; Zhang, L. Z. *J. Mater. Chem.* **2002**, *12*, 81.
(24) Bullen, H. A.; Garrett, S. J. *Nano Lett.* **2002**, *2* (7), 739.
(25) Wang, R.; Sakai, N.; Fujishima, A.; Watanabe, T.; Hashimoto, K. *J. Phys. Chem. B* **1999**, *103*, 2188.
(26) Wandelt, K. *Surf. Sci. Rep.* **1985**, *2*, 1.
(27) Shulz, A. N.; Jang, W. Y.; Hetherington, W. M., III; Baer, D. R.; Wang, L. Q.; Engelhard, M. H. *Surf. Sci.* **1995**, *339*, 114.
(28) Wang, L. Q.; Baer, D. R.; Engelhard, M. H.; Shulz, A. N. *Surf. Sci.* **1995**, *344*, 237.

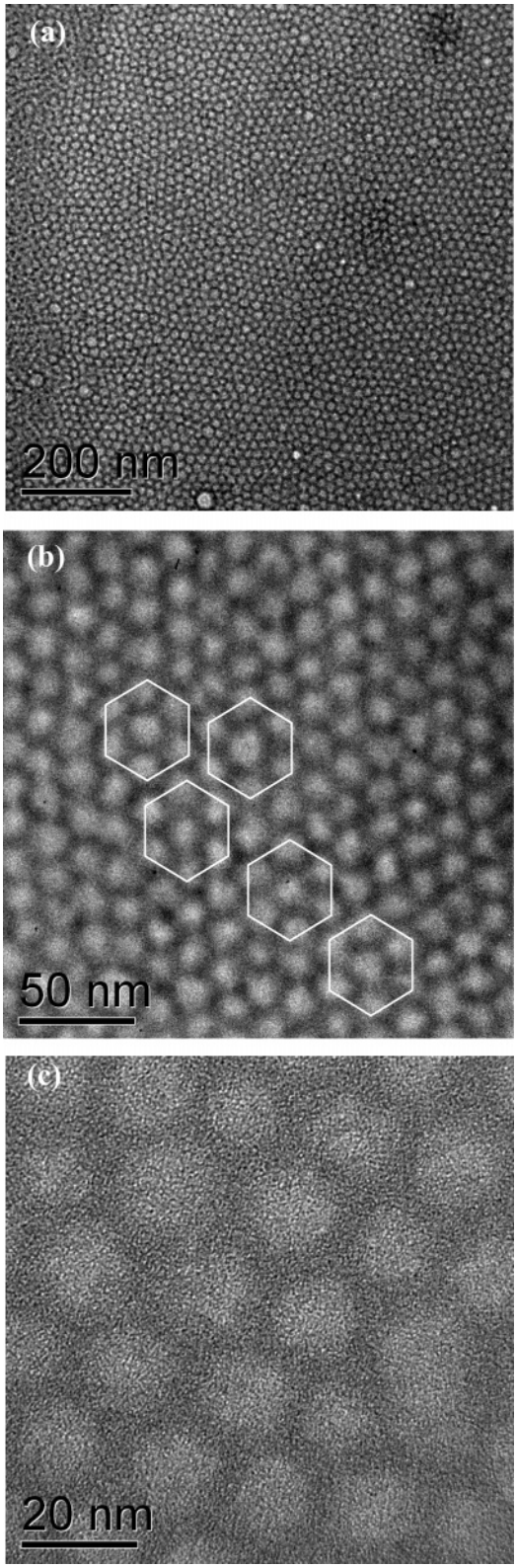

Figure 4. TEM micrographs of the nanohybrid thin film containing titania nanoparticles derived from dissolution of PMMA−PEO diblock copolymer in 50 vol % THF and 50 vol % water at the pH value of 0.33: (a) low and (b,c) high magnifications.

and titania phase. From Figure 4c, it is apparent that the titania corona decorating around these cores are very fine in size, estimated to be <2 nm, creating an interconnected network of inorganic phase rather than discrete nanoparticles. By taking into account the fact that no lattice fringe could be observed in each individual nanoparticle, it can be concluded that the nanocrystallinity of the titania phase is of short range, which is similar to that of the film derived from the precursor solution of pH 1.20.

Annealing Time, Temperature, and Heating Rate. As shown in the previous two sections, both the water content and amount of hydrochloric acid in the solution can strongly affect the nanohybrid structure derived by using poly(methylmethacrylate)-*b*-polyethylene oxide as a template. In addition, the thermal annealing temperature, time, and heating rate are also investigated for their effects on the resulting assembly of nanoparticle arrays. For the nanohybrid thin films discussed above, the duration employed for thermal annealing was considerably long, i.e., 48 h. To investigate the effects of annealing time, the thin film samples were annealed at 150 °C at a heating rate of 1 °C/min for varying durations of 0.5, 1.0, 3.0, and 12 h, respectively. TEM studies show that the film annealed for 0.5 h (Figure 5a) exhibits an irregular stripelike pattern for the PMMA nanodomains, where the fine TiO_2 nanophase was not well-established. Thermal annealing for 1.0 h gave rise to the formation of partially ordered PMMA domains (Figure 5b), although the stripelike feature was still visible in certain local areas. Upon extending the annealing duration to 3.0 h, nanodomains in hexagonal-like configuration were observed (Figure 5c). At this stage, the establishment of titania nanoparticles was also apparent, although the nanoarrays of both organic and inorganic domains were yet fully established. Finally, a well-defined uniformity was achieved for the PMMA domain arrays, which were surrounded by well-interconnected TiO_2 nanoparticles, when the thermal annealing was prolonged to 12 h (Figure 5d). The resulting nanostructures are apparently very similar to those of the thin films annealed for a much longer duration (48 h) as shown in Figure 4b. This suggests that thermal annealing for 12 h is sufficient to complete the self-assembly process for well-organized nanoarrays in the nanohybrid thin film.

The above results of TEM studies can be explained by considering the fact that the initial solution is rather homogeneous since PMMA, PEO, and titanium alkoxide precursor are soluble in the mixed solvent of water and tetrahydrofuran. At this stage, micelles consisting of hydrophilic PEO corona and hydrophobic PMMA core have already formed, although there is little structural arrangement taking place. The formation of cylindrical hydrophobic PMMA domains and the organization of an inorganic titania network in the hydrophilic PEO sites are initiated once the solvent evaporates from thin film, creating a concentration gradient throughout the thickness.[29] With the huge water content, i.e., 50 vol % involved in the mixed solvent, the evaporation rate will be considerably slow. Therefore, upon thermal annealing for a short period of 0.5 h, for example, the resulting nanostructures will retain the disordered features of PMMA−PEO micelles and titanium alkoxide precursor at the solution stage. Increasing the annealing time to 12 h significantly improved the evaporation-induced self-assembly

(29) Grosso, D.; Cagnol, F.; Soler-Illia, G. J. A. A.; Crepaldi, E. L.; Amenitsch, H.; Brunet-Bruneau, A.; Burgeouis, A.; Sanchez, C. *Adv. Funct. Mater.* **2004**, *14*, 309.

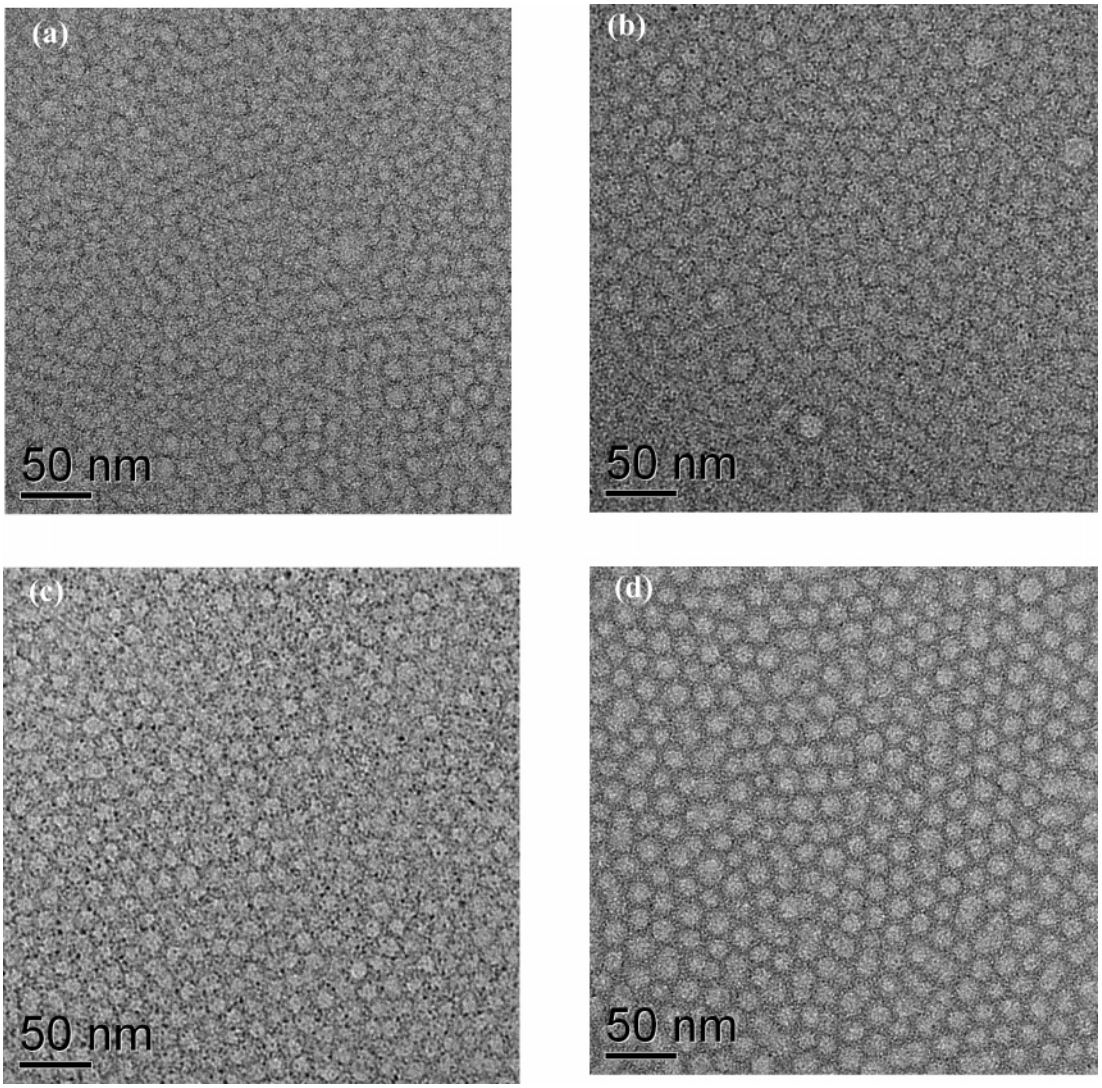

Figure 5. TEM micrographs of the nanohybrid thin films containing titania nanoparticles thermally annealed at 150 °C for (a) 0.5, (b) 1.0, (c) 3.0, and (d) 12 h, respectively, derived from the solution with water content of 50 vol % and pH 0.33.

(EISA) process, leading to a highly ordered arrangement of PMMA and titania nanoparticle domains.

It is of further interest to investigate the feasibility of minimizing the annealing duration by raising the annealing temperature. Indeed, raising the annealing temperature will speed up the self-assembly process by taking into account the enhanced mobility of the polymer chains. In this project, the thermal annealing temperature was varied between 60 and 200 °C, at a fixed duration of 6 h. Figures 6a−6e are the TEM micrographs for the thin films annealed for 6 h at 60, 110, 150, 180, and 200 °C, respectively. At 60 °C (Figure 6a), the arrangement of both PMMA and titania domains was yet established. This was due to the insufficient driving force for self-assembly since the annealing temperature is still far below the glass-transition temperature (T_g) of PMMA, which is ∼105 °C. No regular network of TiO_2 phase could be observed since the inorganic precursor had yet been converted into the desired oxide phase at this stage. The inorganic precursor phase was very much intermixed with the organic template, prevailing randomness among them. Increasing annealing temperature to 110 °C leads to the formation of TiO_2 networks surrounding the PMMA domains, although the arrays of both domains were yet completely built (Figure 6b). As expected, rather ordered, hexagonal-like arrays of titania nanoparticles and PMMA cores were achieved when the annealing temperature was raised to 150 °C (Figure 6c), whereby the difference between the annealing temperature and T_g of PMMA is 45 °C. In comparison to Figure 5c, it shows a more established nanoarray structure, which is indeed similar to the nanostructure shown in Figure 5d. This confirms that a sufficiently high annealing temperature is required to complete the self-assembly process, leading to the establishment of ordered arrays in TiO_2−PMMA nanohybrid thin film. As shown in Figure 6d, annealing at 180 °C for 6 h led to the formation of highly organized and well-aligned hexagonal-like arrays of nanodomains in the TiO_2−PMMA nanohybrid thin film. However, this highly organized nanostructure cannot be maintained when the thermal annealing was performed at 200 °C, where a severe deterioration in the nanoarrays took place (Figure 6e). This suggests that 180 °C ($T - T_g = 75$ °C) is close to the optimized annealing temperature for the self-assembly process, leading to highly aligned arrays of PMMA and TiO_2 nanoparticle domains.

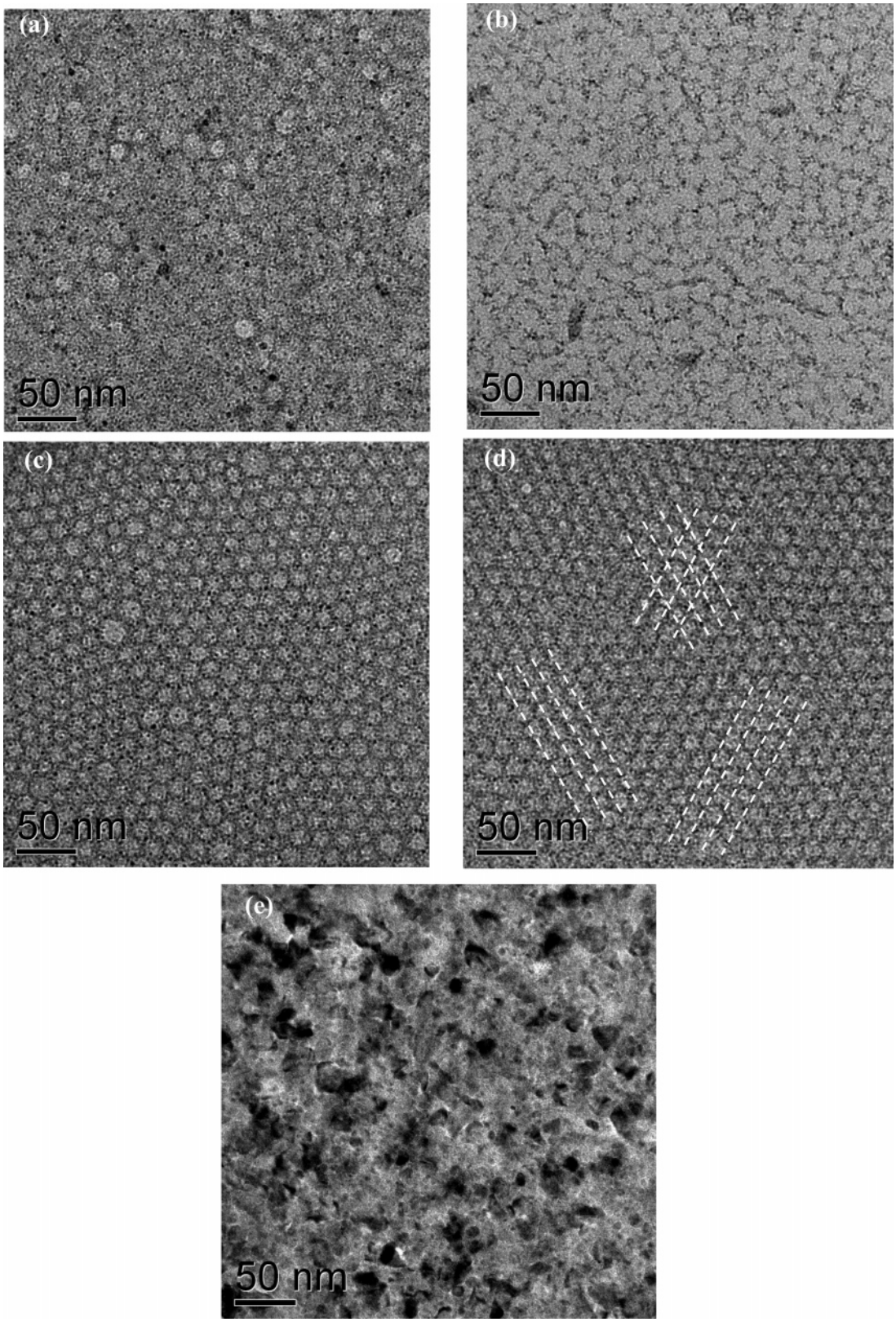

Figure 6. TEM micrographs of the nanohybrid thin film containing titania nanoparticles thermally annealed for 6 h at (a) 60, (b) 110, (c) 150, (d) 180, and (e) 200 °C, respectively, derived from the solution with water content of 50 vol % and pH 0.33.

As shown in Figure 7a, in contrast to the hexagonal-like arrays of PMMA domains and TiO_2 nanoparticles obtained at a heating rate of 1 °C/min, a rather different structure feature resulted when the heating rate was raised to 5 °C/min. The nanohybrid thin film exhibits a nanostructure consisting of clusters of cubical-like arrays. At higher magnifications, the cubical-like arrays (Figure 7b) are shown to consist of titania nanoparticles of ∼7 nm in average size, together with PMMA domains of ∼10 nm in average size.

Post-hydrothermal Treatment. Concerning the lack of nanocrystallinity for the TiO_2 nanoparticles assembled in a

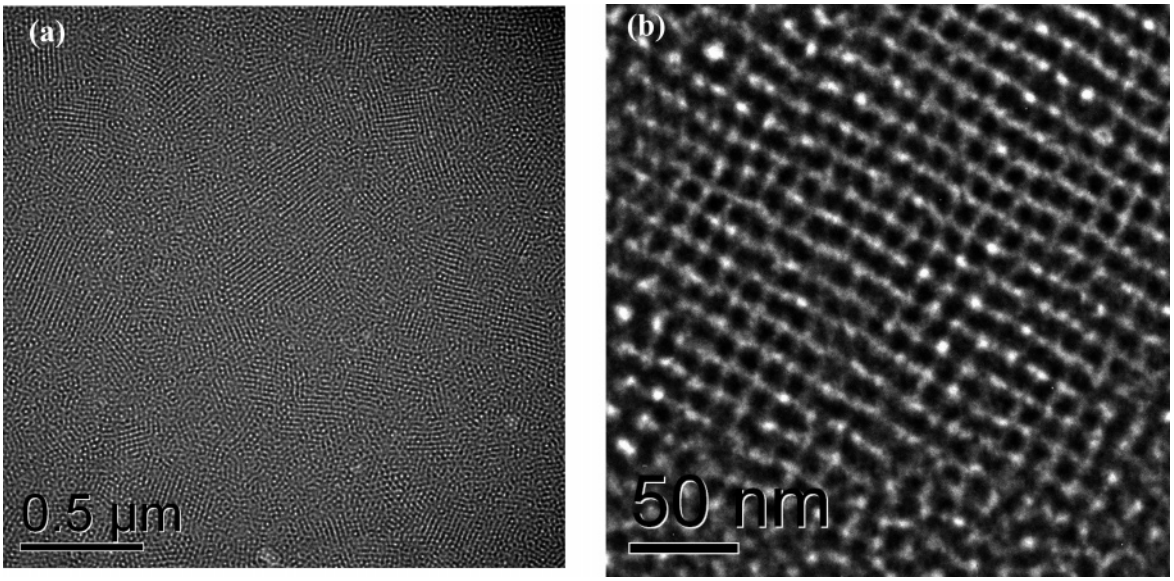

Figure 7. TEM micrographs of the nanohybrid thin film containing titania nanoparticles annealed at 150 °C for 6 h at a heating rate of 5 °C/min derived from the solution with water content of 50 vol % and pH 0.33: (a) low and (b) high magnifications, showing clusters of cubical-like arrays of titania nanoparticles and PMMA cores.

polymer matrix, Brinker and Hurd[30] and Langlet et al.[31] have suggested that the largely amorphous nature is related to the high functionality of the titanium alkoxide precursor favoring the fast development of a stiff Ti−O−Ti network via condensation. In this connection, a further study by Matsuda et al.[32] and Matsuda and co-workers[33] suggested that some structural changes in the TiO_2 thin films derived from sol−gel process could be induced by the treatment in a high-humidity environment at temperatures above 100 °C. Further investigation by Imai et al.[34] and Imai and Hirashima[35] confirmed that the exposure of sol−gel-derived TiO_2 films to water vapor triggered rearrangement of the Ti−O−Ti network, leading to the formation of anatase phase at relatively low temperature (180 °C). On the basis of this understanding, we have investigated the feasibility of enhancing the nanocrystallinity of TiO_2 phase assembled by diblock copolymer templating by a post-hydrothermal process. For this, the thin films spin-coated on glass substrates were first annealed at 150 °C for 48 h and then exposed to the treatment by high-pressure water vapor in a Teflon-lined stainless steel autoclave (Parr, Moline, IL) at 150 °C for 24 h. A specially designed stand was placed inside the Teflon tube to prevent the samples from direct contact with liquid water. A high-magnification TEM micrograph for the post-hydrothermally treated film is given in Figure 8a. The film clearly shows crystallites with well-established lattice fringe. The *d*-spacing of the lattice fringe is measured to be 0.352 ± 0.008 nm, which is in good agreement with the *d*-value of the (101) crystal plane in anatase titania. According to the model by Imai and co-workers,[34,35] the enhancement in TiO_2 crystallinity involves the cleavage of strained Ti−O−Ti bonds by water molecules, resulting in the formation of much more flexible Ti−OH, leading to the rearrangement and densification of ordered Ti−O−Ti bonds. As a consequence of the crystallite growth, the well-organized arrays of individual core-corona structures in the hexagonal-like or cubical-like configurations have undergone some rearrangement. However, when observed at low magnification (Figure 8b), it is obviously seen that the orderly arrangement by diblock copolymer templating can be maintained to some extent at large scales, where the TiO_2 nanocrystallites are dispersed quite uniformly in the polymer matrix. This suggests that under a well-controlled post-hydrothermal treatment condition, it would be possible to obtain nanohybrid thin film containing highly ordered arrays of TiO_2 nanoparticles in the hexagonal-like or cubical-like configurations, while at the same time they are of enhanced crystallinity.

Figures 9a and 9b show the high-resolution XPS spectra of the O 1s region for the conventionally annealed and post-hydrothermally treated nanohybrid samples, TEM micrographs of which have been shown in Figures 4c and 8a, respectively. Both spectra demonstrate broad and asymmetric signals ranging from ∼526 to 536 eV, indicating the coexistence of different chemical environments on the titania nanoparticle surfaces. Each spectrum can be fitted into three peaks located at ∼529.5−530, 531.5 ± 0.5, and 533 ± 1 eV, attributed to oxygen in the metal oxide component (i.e., O^{2-} bound to Ti^{4+} in the TiO_2 lattice), oxygen in the hydroxyl groups (−OH) or defective oxides, and physisorbed or chemisorbed molecular water, respectively.[36] The last two species are mainly associated with the TiO_2 surfaces. In the conventionally annealed sample (Figure 9a), the estimated area percentage under the metal oxide peak was ∼23.04%, which is considerably lower than that of the hydroxyl groups/defective oxides (∼63.46%). This is in agreement with the

(30) Brinker, C. J.; Hurd, A. J. *J. Phys. III France* **1994**, *4*, 1231.
(31) Langlet, M.; Burgos, M.; Couthier, C.; Jimenez, C.; Morant, C.; Manso, M. *J. Sol−Gel. Sci. Technol.* **2001**, *22*, 139.
(32) Matsuda, A.; Kotani, Y.; Kogure, T.; Tatsumisago, M.; Minami, T. *J. Am. Ceram. Soc.* **2000**, *83* (1), 229.
(33) Kotani, Y.; Matsuda, A.; Kogure, T.; Tatsumisago, M.; Minami, T. *Chem. Mater.* **2001**, *13*, 2144.
(34) Imai, H.; Moromoto, H.; Tominaga, A.; Hirashima, H. *J. Sol−Gel Sci. Technol.* **1997**, *10*, 45.
(35) Imai, H.; Hirashima, H. *J. Am. Ceram. Soc.* **1999**, *82* (9), 2301.
(36) Sanjines, R.; Tang, H.; Berger, H.; Gozzo, F.; Margaritondo, G.; Levy, F. *J. Appl. Phys.* **1994**, *75* (6), 2945.

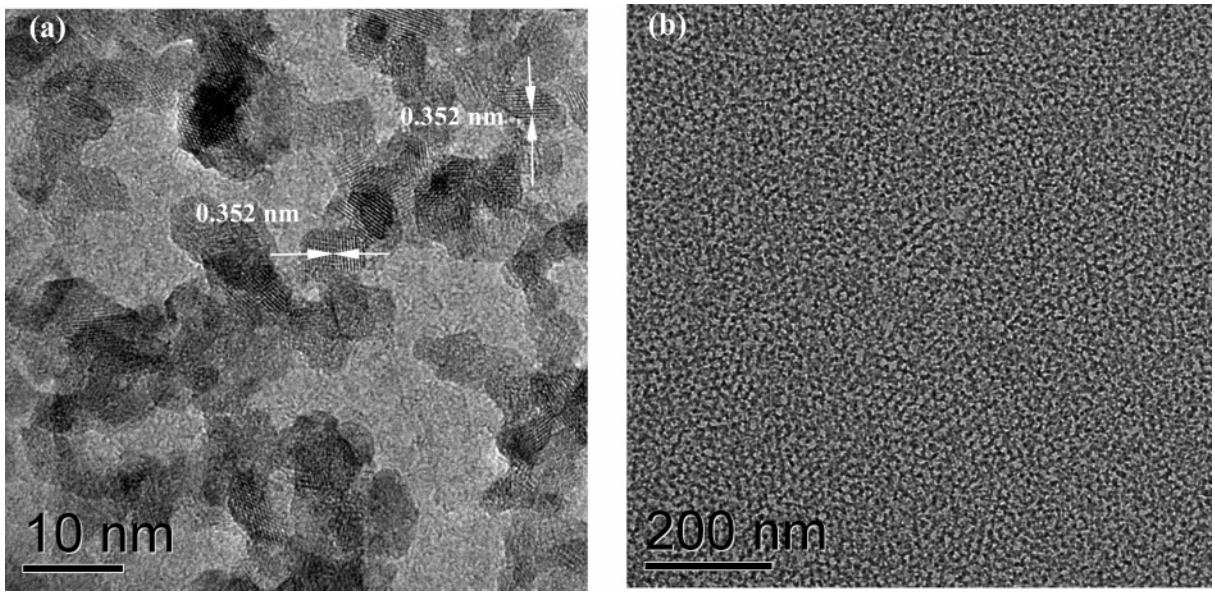

Figure 8. TEM micrographs of the nanohybrid thin film containing titania nanoparticle arrays derived from the solution with water content of 50 vol % and pH 0.33 upon post-hydrothermal treatment showing (a) well-established lattice fringe in the crystallites and (b) well-dispersed TiO_2 nanocrystallines in the PMMA matrix.

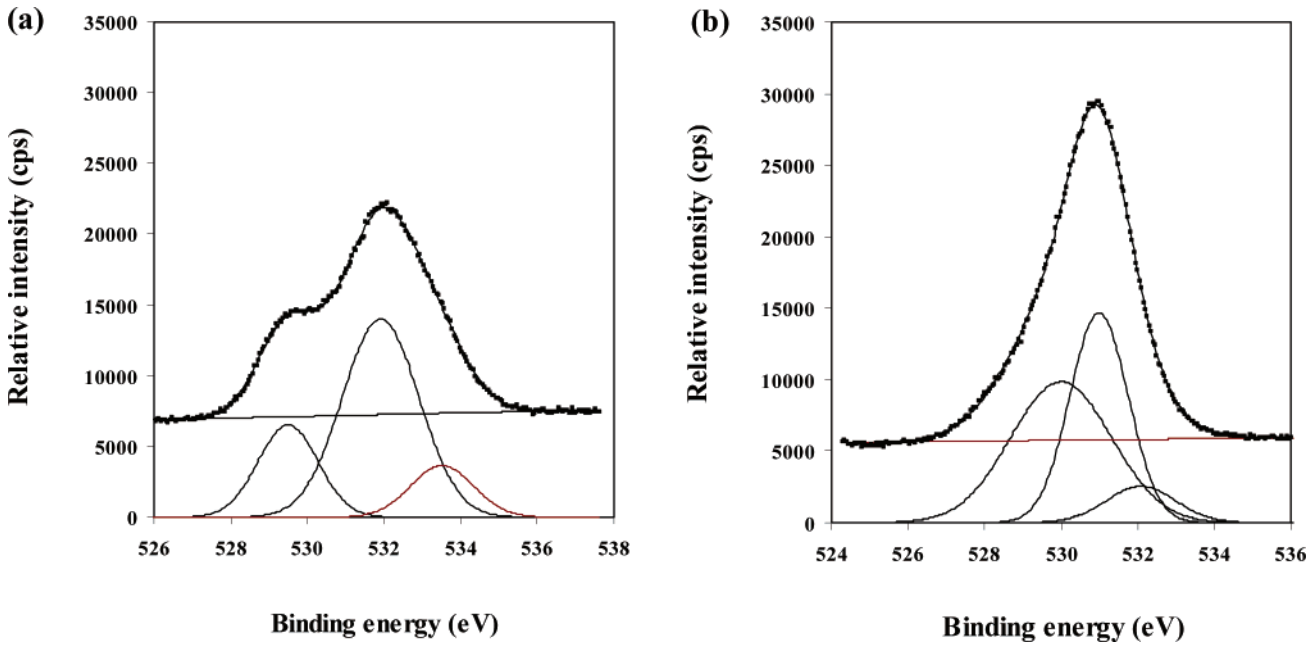

Figure 9. XPS high-resolution O 1s spectra of (a) the conventionally annealed and (b) the post-hydrothermally treated nanohybrid thin film containing titania nanoparticle arrays in PMMA matrix, derived from the solution with water content of 50 vol % and pH 0.33.

fact that the TiO_2 phase in this sample is still largely amorphous, as has been shown by the XRD and TEM studies. Due to the strained characteristics of Ti−O−Ti bonds contained in the hydroxyl groups as well as the nonstoichiometric nature of the defective oxides, a retardation toward formation of a well-crystallized TiO_2 phase is therefore expected. On the other hand, when the hydrothermal treatment was applied to the thin film sample, the percentage of metal oxide peak increases significantly up to ∼49.02%, accompanied by a decrease in the hydroxyl-defective oxides peak down to ∼42.28% (Figure 9b). This confirms the effectiveness of high-pressure water vapor in converting the surface states of TiO_2 nanoparticles to less defective ones, promoting the crystallinity. Similar results on the role of water vapor in removing the surface defects have been reported for bulk TiO_2 (110) surfaces by Wang et al. [28] It is also observed that there occurs a reduction of chemisorbed water content from 13.50% to 8.69%, which is believed to be a consequence of the involvement of water molecules in the cleavage of the strained Ti−O−Ti bonds and their rearrangements into crystalline TiO_2 phase.

Further confirmation on the post-hydrothermal treatment in promoting the nanocrystallinity of nanohybrid film is given by FTIR results in Figure 10. The hydroxyl groups of Ti−OH in the spectra of the conventionally annealed and post-hydrothermally treated samples are observed as a broad absorption band in the range of ∼3400−3500 cm^{-1},[37] while the characteristic peak for TiO_2 phase is indicated by a

(37) Lee, L. H.; Chen, W. C. *Chem. Mater.* **2001**, *13*, 1137.

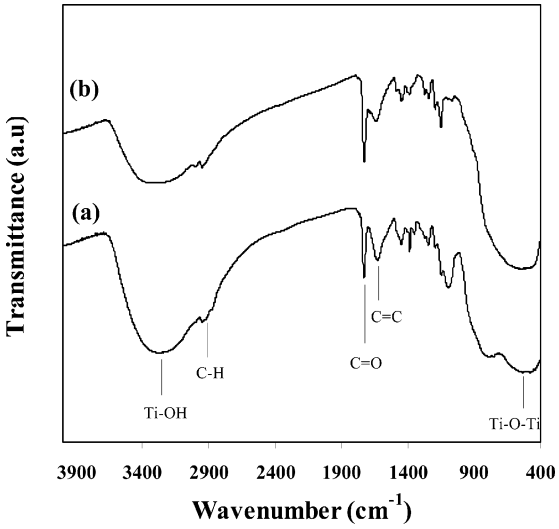

Figure 10. FTIR spectra of (a) the conventionally annealed and (b) the hydrothermally treated nanohybrid thin film, derived from the solution with water content of 50 vol % and pH 0.33.

vibration band of Ti−O−Ti groups at 900−400 cm^{-1}.[38] Apparently, the conventionally annealed thin film shows a more intense Ti−OH band than that of the post-hydrothermally treated sample, while on the other hand the latter demonstrates a stronger intensity for Ti−O−Ti band than the former. This is consistent with the results of TEM and XPS studies, showing that the post-hydrothermally treated sample exhibits an enhanced nanocrystallinity of TiO_2 phase.

From the surface profiler measurement, it was observed that there was a change in film thickness. It was initially 36 nm for the conventionally annealed sample, while the post-hydrothermal treatment reduced it to 24 nm. This indicates that part of the film surface was leached out by the water molecules at high vapor pressure. On the other hand, however, it was also observed that the stretching vibration bands of C═O and C−H in the PMMA segments at 1730 and 2950 cm^{-1} on both samples are almost the same in intensity. It suggests therefore that the internal integrity of the polymer chains in the PMMA matrix is successfully retained. A longer duration (48 h) for the initial conventional annealing prior to hydrothermal treatment was able to stabilize the polymer chains in the nanohybrid thin film.

UV−Vis and Photoluminescence Spectra. The TiO_2−PMMA nanohybrid thin films derived from conventional in situ sol−gel and polymerization routes were previously studied for optical properties.[39] Their linear and nonlinear optical properties are greatly affected by the nanocrystallinity of TiO_2 particles, in addition to the particle size and size distribution. UV−vis and photoluminescence spectroscopies are conducted in the present work for the nanohybrid thin films derived from diblock copolymer templating. The effects of crystallinity on the optical properties of the TiO_2−PMMA nanohybrid thin films derived from diblock copolymer templating is shown in Figure 11a, where the UV−vis absorption spectra are plotted for the conventionally annealed and post-hydrothermally treated nanohybrid thin films. Both thin films are highly transparent in the visible region. However, it is clearly seen that absorbance of the latter is higher than the former. Further careful comparison between the spectra shows that the conventionally annealed film exhibits an onset of the absorbance edge at about 360 nm in wavelength, while for the post-hydrothermally treated film, it is rather red-shifted to a higher wavelength of about 380 nm. With use of Tauc et al.'s equation,[40] a plot of $(\alpha h\nu)^{1/2}$ versus $h\nu$ is given in Figure 11b, where the extrapolation of linear parts of the curves to the energy axis provides an estimated band gap energy, E_g of 3.34 and 3.21 eV for the conventionally annealed and post-hydrothermally treated nanohybrids, respectively. The latter demonstrated an E_g comparable to that of pure anatase TiO_2 thin films, which is in the range of 3.20−3.23 eV.[41] This confirms the enhanced nanocrystallinity of TiO_2 nanoparticles in this sample, as has been confirmed by TEM, XPS, and FTIR studies. On the other hand, a blue shift of approximately 0.14 eV relative to the bulk E_g value of anatase titania is evident for the conventionally annealed film, which was confirmed to be rather amorphous. By taking into account the fine nanoparticles in this sample, one can conclude that such a blue shift is mainly due to the quantum size effect, as has been observed in many nanostructured semiconductor materials.[42]

It is well-known that TiO_2, as an indirect band gap semiconductor, does not show luminescence under normal conditions, although it has demonstrated some luminescent behavior, for instance, in a vacuum environment,[43] at very low temperature,[44] in the presence of dopant,[44] or in ultrafine TiO_2 colloidal solution form.[45] Figure 12 shows the photoluminescence behavior of the conventionally annealed and post-hydrothermally treated nanohybrid thin films under excitation with $\lambda = 325$ nm in air at room temperature. Both spectra demonstrate a very similar feature but they are different in terms of intensity. In general, the conventionally annealed thin film shows a higher intensity photoluminescence spectrum than the post-hydrothermally treated thin film. Both samples demonstrate a strong band appearing at 350−475 nm, which is assigned to the characteristic emission of free excitons in the anatase titania.[46] Another broadband is present at 475−650 nm, which is related to the emission of self-trapped states bound to the defect state induced by coordinated surface groups.[47] Banyai et al.[48] suggested that self-trapped states via binding to surface defect states can be formatted constructively through the quantum confinement and dielectric confinement effects. In addition, it has been

(38) Wang, S. X.; Wang, M. T.; Lei, Y.; Zhang, L. D. *J. Mater. Sci. Lett.* **1999**, *18*, 2009.
(39) Yuwono, A. H.; Liu, B. H.; Xue, J. M.; Wang, J.; Elim, H. I.; Ji, W.; Li, Y.; White, T. J. *J. Mater. Chem.* **2004**, *14*, 2978.
(40) Tauc, J.; Grigorovich, R.; Vancu, A. *Phys. Status Solidi* **1966**, *15*, 627.
(41) Wang, Z.; Helmersson, U.; Käll, P. O. *Thin Solid Films* **2002**, *405*, 50.
(42) Wu, X. C.; Zhou, B. S.; Xu, J. R.; Yu, B. L.; Tang, G. Q.; Zhang, G. L.; Chen, W. J. *Nanostruct. Mater.* **1997**, *8*, 179.
(43) Forss, L.; Schubnell, M. *Appl. Phys. B* **1993**, *56*, 363.
(44) Tang, H.; Berger, H.; Schmid, P. E.; Levy, F. *Solid. State. Commun.* **1993**, *87*, 847.
(45) Liu, Y. J.; Claus, R. O. *J. Am. Chem. Soc.* **1997**, *119*, 5273.
(46) Zhu, Y. C.; Ding, C. X. *J. Solid State Chem.* **1999**, *145*, 711.
(47) Wang, Y.; Zhang, S.; Wu, X. *Nanotechnology* **2004**, *15*, 1162.
(48) Banyai, L.; Gilliot, P.; Hu, Y. Z.; Koch, S. W. *Phys. Rev. B* **1992**, *45*, 14136.

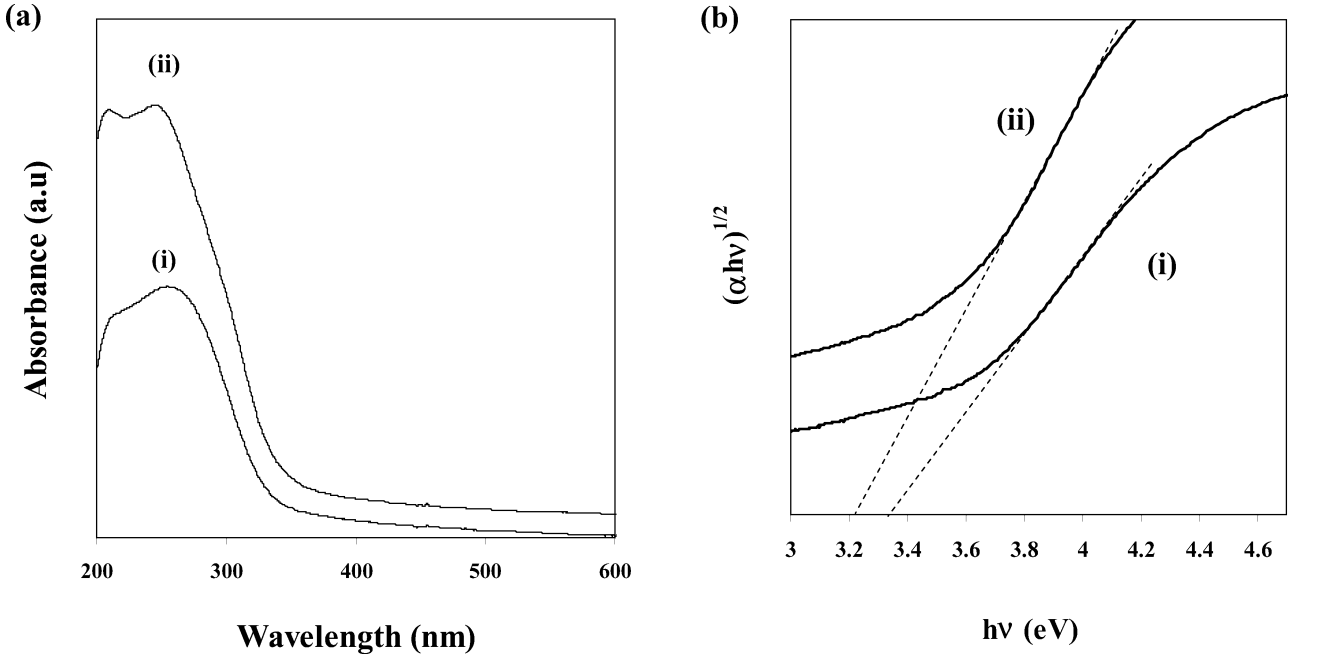

Figure 11. (a) UV−Vis spectra of (i) the conventionally annealed and (ii) the hydrothermally treated nanohybrid thin film, derived from the solution with water content of 50 vol % and pH 0.33. (b) Corresponding band gap energy, E_g, for samples (i) and (ii), respectively, estimated by using Tauc's equation.

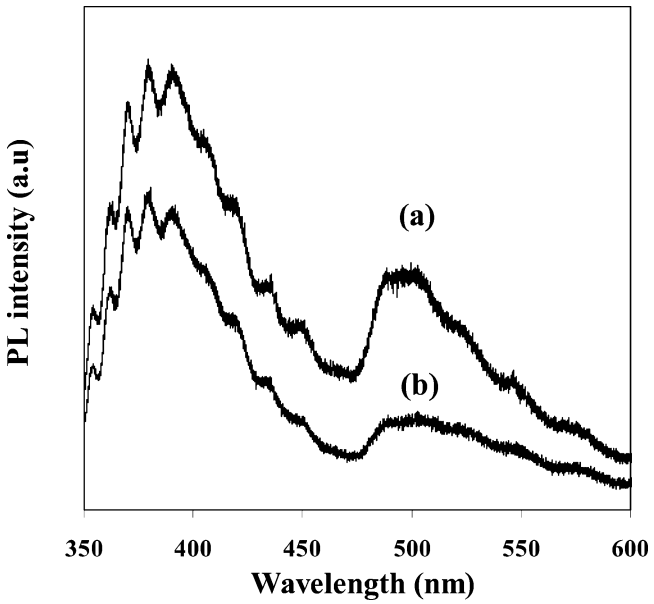

Figure 12. Photoluminescence spectra of (a) the conventionally annealed and (b) the hydrothermally treated nanohybrid thin film, derived from the solution with water content of 50 vol % and pH 0.33.

shown by Zhou et al.[49] that the interfacial effect between the titanium dioxide and the surfactant plays an important role in light emission. It has also been reported that the photoluminescence spectra of anatase titania in general can be attributed to three types of origins, namely, surface states,[43] self-trapped excitons,[44,50] and oxygen vacancies.[50,51] According to the XPS result of the O 1s region shown in Figure 9, it can apparently be seen that the content of defective oxides in the conventionally annealed thin film is larger than that of the post-hydrothermally treated thin film. The Ti_2O_3 phase included in the defective oxides thus play an important role as surface defect species for the emission of self-trapped excitons in the observed photoluminescence spectra. It explains why the conventionally annealed thin film demonstrates a higher photoluminescence intensity than that of the post-hydrothermally treated sample.

Conclusions

A solvent modification enables PMMA−PEO diblock copolymer to be used as a template for synthesizing nanohybrid thin film containing highly ordered arrays of TiO_2 nanoparticles in PMMA matrix. Desirable nanohybrid structures were derived by dissolving the block copolymer in a mixture solvent consisting of 50 vol % water in THF. At a pH level of 0.33, the undesired premature precipitation of TiO_2 precursor is prevented, despite the high water content involved. This gave rise to a nanohybrid thin film consisting of PMMA domains in hexagonal-like configuration surrounded by very fine titania nanoparticles of ∼2 nm in size. Raman spectroscopy confirms the formation of anatase as the predominant inorganic phase in the nanohybrid, where TiO_2 dominates the interior structure of the nanoparticles, as shown by the Ti 2p spectrum of XPS analysis, although there is a possibility that certain Ti_2O_3 defect species can be formed on the nanoparticle surfaces. Several processing parameters including the annealing temperature, time, and heating rate have been shown to strongly affect the resulting nanostructure and nanoparticle arrangement in the nanohybrid thin films. Increasing the heating rate up to 5 °C/min effectively leads to the conversion from a hexagonal-like to a cubical-like hierarchical structure, accompanied by a significant increase in the nanoparticle size of titania phase, up to ∼7 nm. A post-hydrothermal treatment in high-pressure water vapor significantly enhances the crystallinity of TiO_2 nanoparticles, although it triggers a structural rearrangement,

(49) Zhou, B. S.; Xiao, L. Z.; Li, T. J.; Zhao, J. L.; Gu, S. W. *Appl. Phys. Lett.* **1991**, *59*, 1826.
(50) Saraf, L. V.; Patil, S. I.; Ogale, S. B.; Sainkar, S. R.; Kshisarger, S. T. *Int. J. Mod. Phys.* **1998**, *12*, 2635.
(51) Serponne, N.; Lawless, D.; Khairutdinov, R. *J. Phys. Chem.* **1995**, *99*, 16646.

due to the growth of TiO_2 nanocrystallites. As a consequence of the enhanced nanocrystallinity, the hydrothermally treated nanohybrid film exhibited a higher absorption in the visible region and a red shift in the absorbance edge toward higher wavelength in the UV region, when compared to that of the conventionally annealed thin film. The band gap energy of the hydrothermally treated nanohybrid film was calculated to be 3.21 eV, which is close to that of bulk anatase titania. On the other hand, the hydrothermal treatment led to a lower photoluminescence intensity, in comparison to the conventionally annealed nanohybrid thin film. This is consistent with the observation that the former contained less defective oxides than that of the latter, as confirmed by XPS analysis in the O 1s region.

CM061495F